Phase transitions in Sr_2YRuO_6 investigated by Mössbauer spectroscopy, magnetization, and thermodynamic measurements

G. Long,[1] M. DeMarco,[1,2] D. Coffey,[2,*] M. K. Toth,[3] and M. S. Torikachvili[3]
[1]*Department of Physics, State University of New York at Buffalo, Buffalo, New York 14260, USA*
[2]*Department of Physics, Buffalo State College, Buffalo, New York 14222, USA*
[3]*Department of Physics, San Diego State University, San Diego, California 92182, USA*
(Received 4 September 2012; revised manuscript received 23 December 2012; published 22 January 2013)

Recent specific-heat data measured in Sr_2YRuO_6 have revealed two transition features at ∼26 and ∼30 K, where only one transition could be inferred before from magnetic susceptibility and transport measurements. We have investigated this temperature region using ^{99}Ru Mössbauer spectroscopy, magnetization, and thermodynamic measurements in order to elucidate the unusual properties in this temperature region. Below 25 K, fits to the Mössbauer spectra show that there is a unique value of the hyperfine magnetic field at each Ru site indicating static long-range magnetic order. Beyond 25 K, this static long-range magnetic order rapidly deteriorates. We have found that the temperature dependence of the Mössbauer spectra between ∼25 and ∼28 K can be described as due to either motional narrowing or to a temperature-dependent distribution of hyperfine magnetic fields. The Mössbauer spectra collapse to a single peak in this narrow temperature interval so that there is no evidence of static magnetic order by ∼30 K. As a result, no evidence of the transition at 30 K is seen in the Mössbauer spectra.

DOI: 10.1103/PhysRevB.87.024416 PACS number(s): 76.80.+y, 75.50.Ee, 74.70.Pq

I. INTRODUCTION

The first detailed study of the M_2LnRuO_6 (M = Ca, Sr, Ba, and Ln = Y, La, Eu) ruthenium perovskites was carried out by Greatrex *et al.*[1] who determined crystal structure, measured the temperature dependence of the electrical resistivity and magnetic susceptibility, and the ^{99}Ru Mössbauer effect (ME) at 4.2 K. They found that these materials have a monoclinic $P2_1/n$ space group and are magnetically ordered at 4.2 K with hyperfine magnetic fields B_{hf} at the Ru sites between ∼56 and ∼59.5 T due to the electronic magnetic order. The structure of these materials is similar to that of $SrRuO_3$ except that half the Ru are replaced by Ln. Sr_2YRuO_6 is representative of this class of ruthenates which are local-moment antiferromagnetic insulators at low temperatures. The lower symmetry compared to $SrRuO_3$ comes from the difference in ionic radius of Ru and the Ln. The six-coordinate ionic radius of Ru is 0.565 Å, whereas that of Y is 0.90 Å. This results in larger bond lengths in the YO_6 octahedra than in the RuO_6 octahedra and rotations of the octahedra. The same large discrepancy in ionic radii holds when Y is substituted with any of the rare-earth lanthanides. The same space group is seen in Sr_2LnRuO_6, where Ln = Eu-Lu, except that there are moments on the Ln sites.[2,3] The Sr_2LnRuO_6 have magnetic transitions with values of T_N almost independent of Ln.

Battle and Macklin[4] found that the Ru moments at T = 4.2 K lie in the YRuO planes in Sr_2YRuO_6 using neutron diffraction. The Ru moments form ferromagnetic (001) sheets which are coupled antiferromagnetically along [001], perpendicular to the YRuO planes. This configuration is one of the classical ground states of the nearest-neighbor Heisenberg model on a face-centered-cubic (fcc) lattice, where each moment has 12 nearest neighbors. Each moment couples ferromagnetically to four neighbors in its YRuO sheet and antiferromagnetically with eight nearest neighbors in the two neighboring sheets. The magnitude of the ordered Ru moment is 1.85 μ_B per Ru^{5+} ion and even modest applied magnetic fields, ∼3.8 T, resulted in a spin-flop transition below ∼12 K. This suggests the presence of a small degree of magnetic anisotropy which would prevent the moments responding to small applied magnetic fields, but which is overcome at modest field strengths.

Cao *et al.*[5] found magnetic order occurring below 26 K in single-crystal samples of Sr_2YRuO_6 in agreement with the results on polycrystalline samples. They measured magnetization and resistivity as a function of temperature and applied magnetic field. Unlike Battle and Macklin, they did not find evidence of a spin-flop transition, although they found that the transition to magnetic order broadened in an applied field, which is characteristic of a ferromagnet. They also found hysteresis at low temperatures consistent with a small net ferromagnetic component, which they attributed to canting of the Ru moments.

The recent upsurge of interest in Sr_2YRuO_6 so many years after the original work is due in part to claims of superconductivity when it is doped with Cu.[6–9] However, this finding is controversial.[10,11] ^{99}Ru Mössbauer data on $SrYRu_{.95}Cu_{.05}O_6$ clearly show a large hyperfine magnetic field, ∼60 T, which is very similar to the value reported here by us in Sr_2YRuO_6, while the sample was reported to have a superconducting transition with an onset at 45 K. This apparent coexistence of magnetic order, with $T_N \simeq 26$ K, and superconductivity is reminiscent of that seen in $RuSr_2GdCu_2O_8$, except that T_N is greater than T_{SC} in that case. Wu *et al.*[7] also reported superconductivity in $Sr_2Ho(Ru_{1-x}Cu_x)O_6$. Although there is no microscopic model for this coexistence of these phases in $RuSr_2GdCu_2O_8$, there are distinct CuO and RuO planes and the two types of order are thought to exist in the two different structural components. Since there is no CuO layer in $SrYRu_{.95}Cu_{.05}O_6$, it is even more of a challenge to understand the coexistence of these two phases in this material. Harshman *et al.*[9] claim that the SrO layer between the YRuO planes in Sr_2YRuO_6 becomes superconducting. However, Galstyan *et al.* have suggested that the superconducting signal comes from $YSr_2Cu_3O_{7-\delta}$ or $YSr_2Cu_{3-x}Ru_xO_{7-\delta}$ impurity

phases.[10,11] The effect of doping was also investigated in $Sr_2EuRu_{1-x}Cu_xO_6$[12] and $Ba_2EuRu_{1-x}Cu_xO_6$[13] with $x \leqslant 0.2$ using the ^{151}Eu ME. The large transferred hyperfine field at the Eu site showed that these materials remained magnetically ordered with unchanged T_N throughout the doping range, but no evidence of superconductivity was reported.

Singh and Tomy[14] measured magnetization and specific heat of polycrystalline samples of Sr_2YRuO_6 and found evidence of two transitions, one at ∼26 K, which previous authors attributed to the transition from magnetic order, and a second at ∼32 K, which had not been previously known. They attributed both transitions seen in the specific heat to magnetic transitions of Ru^{+5} moments.

The goal of this investigation was to probe the magnetic properties in this temperature range. In the course of our investigations, we observed that magnetic order rapidly deteriorates beyond ∼26 K in the samples which we measured and by ∼30 K there is no evidence of static magnetic order. Therefore, the transition at ∼30 K, seen in the specific heat, can not be associated with a transition from static magnetic order. In the model of Singh and Tomy, there are two components to the magnetic order with oppositely aligned net ferromagnetic moments. These components would each lead to different hyperfine fields on the Ru sites, which is not seen in the Mössbauer spectra (MS) reported here. More recently, Bernardo *et al.*[15] have shown that the two peaks in the specific heat correlate very well in temperature with the two features in the thermal expansion of Sr_2YRuO_6. The two features in thermal expansion correspond to subtle structural modifications that were not identified in the previous x-ray and neutron diffraction studies. They also identified these peaks with an increase in the distance between the Ru atoms and in-plane O atoms which Ru shares with the YO_6 octahedra and the Ru-O-Y angle at ∼24 K and a decrease in this distance and angle at ∼30 K from the temperature dependence of their high-resolution x-ray powder diffraction data.

We have analyzed the transition from static magnetic order above ∼26 K in terms of two models which provide equally satisfactory fits to the MS. One model describes the data in terms of motional narrowing, where the hyperfine magnetic field randomly switches direction at a rate which increases with temperature. In the other model, microscopically large domains of static magnetic order break up for $T > 26$ K, leading to a distribution of B_{hf} which evolves with temperature so that the average $B_{hf} \simeq 7$ T at 28 K. Comparison with recent neutron scattering data[16] suggests that motional narrowing is the most likely explanation.

II. EXPERIMENTAL TECHNIQUES

A. Sample synthesis

The samples were synthesized by solid reaction. The starting materials were high-purity powders of $SrCO_3$, Y_2O_3, and 96.63% enriched ^{99}Ru from Oakridge National Laboratory. The powders were ground together thoroughly and reacted at 950 °C in air for a few days, with several intermediate regrindings. The reacted powders were pelletized and fired again in air at 1250 °C for a few days. The x-ray powder diffraction analysis showed a minute amount of impurity phases, and the fits to the MS suggested the presence of a small amount of RuO.

B. Thermodynamic measurements

Measurements of specific heat and magnetic susceptibility as a function of temperature, and magnetization curves, were carried out in a Physical Property Measurement System (PPMS) by Quantum Design equipped with a 9 T magnet, using a relaxation calorimeter and a vibrating sample magnetometer, respectively.

C. Mössbauer experiments

The ^{99}Ru ME was performed by producing a 25 mCi source of ^{99}Rh(Ru) by proton bombardment in a cyclotron on enriched isotope targets as described in a previous paper.[17] The experiments were performed in two cryostats (detailed below), both in transmission geometry. The calibration of the spectrum was determined by the inner four lines of a ^{57}Co(Rh) source versus an α-Fe foil, while the zero velocity was determined by the ^{99}Rh(Ru) versus Ru powder experiment. In the smaller zero magnetic field Janis cryostat, the 1 cm diameter samples containing about 70 mg/cm^2 of enriched ^{99}Ru were mounted in aluminum sample holders, which were attached to a brass ring that was wrapped with heating wire to enable temperature variation. Both the source and absorber were kept at nearly the same temperature by the helium exchange gas in the sample chamber. The temperature was maintained by a Lakeshore temperature controller and diode to within $\frac{1}{4}$ K. The operation of the Mössbauer probe and detector for the zero magnetic field cryostat has been described previously in other studies.[17]

In the larger Janis cryostat with a 9 T superconducting magnet, the Mössbauer probe fits into the sample chamber and was constructed using G10 tubing. The Mössbauer transducer at the top of the cryostat was connected to two concentric G10 tubes of different diameters connected together near the source by a centering two-dimensional spring. The inner tube was fixed to the source and the outer tube held to the sample to be studied. The sample was positioned below the source in the center of the superconducting solenoid magnet and contained about 70 mg/cm^2 of enriched ^{99}Ru in a 1 cm diameter aluminum sample holder.

The source is in a nearly zero magnetic field produced by a magnetic canceling coil at the top of the magnet. In the experiments, the applied magnetic field is parallel to the direction of propagation of the incident γ ray. The detectors used with this larger cryostat were 12 in. from the source for the ^{99}Ru Mössbauer effect. The velocity calibration and zero velocity were determined as described elsewhere.[17] The detector for the ^{99}Ru ME was a $\frac{1}{4}$ in. thick NaI detector set below the bottom of the cryostats Mylar window. When the superconducting magnet was in operation, magnetic shielding was necessary because the NaI detector was in approximately 0.01 T magnetic field due to the fringe fields of the superconducting magnet. This magnetic field was present even though a canceling coil was used at the bottom of the superconducting coil. The NaI detector and base were wrapped in concentric magnetic shielding cylinders (with caps on either end), each of 0.065 in. thick FeSi and Mu metal. The caps at the top of the cylinder had

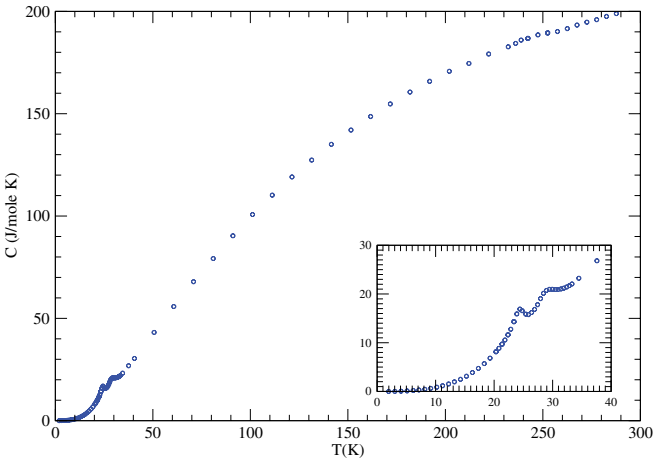

FIG. 1. (Color online) Specific heat with transitions at ∼26 and ∼30 K.

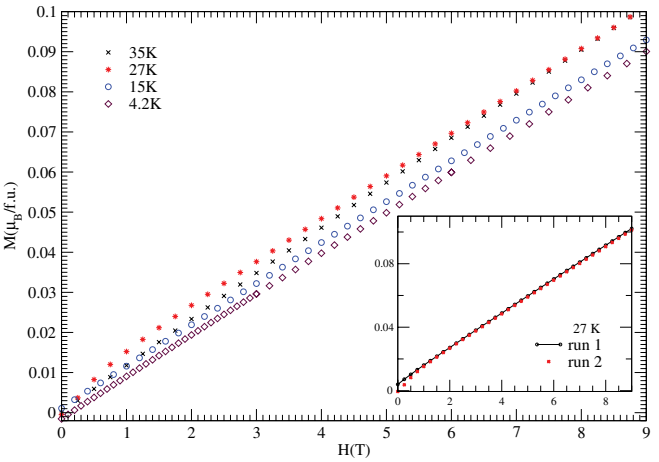

FIG. 3. (Color online) Magnetization versus applied field.

a 1 in. diameter hole to allow the γ ray to enter the NaI detector. The magnetic shielding allowed the NaI detector to operate in up to 5 T external fields from the superconducting magnet. To our knowledge, measurements of the ^{99}Ru ME have not previously been performed in 3 and 5 T magnetic fields. The temperature in the large cryostat was maintained by passing helium gas through a needle valve from the liquid-helium reservoir into the sample chamber from the bottom of the cryostat, which then drifts upward to the sample. Two Cernox thermometers, one at the sample holder and one at the bottom of the chamber, were used for temperature measurements and were controlled by a Lakeshore temperature controller.

III. RESULTS

A. Thermodynamic measurements

The specific heat, shown in Fig. 1, shows two features centered near ∼26 and ∼30 K. The field-cooled magnetic susceptibility data (Fig. 2) show a prominent broad symmetric peak near ∼26 K [inset (a)], which starts to develop at 20 K and dies out at 32 K. This broad peak is similar to the field-cooled temperature dependence reported by Singh and Tomy.[14] The Curie-Weiss fit [inset (b)] gives $\mu_{\rm eff} = 4.15\mu_B$, which lies between the expected values for the $+4$ and $+5$ Ru charge states. The value of Θ found in the Curie-Weiss fit is -380 K. This is larger than -140 K found by Greatrex *et al.*[1] who also worked with powdered samples. The difference in values may be due to the scatter in their data which also allow for an intercept closer to the value found here. The Θ value from $(M/H)^{-1}$ versus T data at high temperature for a single crystal with the applied magnetic field in the ab plane was -2.5 K. This is consistent with weak ferromagnetism. It is likely that the main contribution to the large and negative value of Θ found in polycrystalline samples comes from the field orientation in the c direction, along the direction in which Ru moments alternate orientation. The magnetization as a function of applied magnetic field is shown in Fig. 3 for a range of temperatures. The spin-flop transition reported by Battle and Macklin[4] is not seen. This is in agreement with the work of Cao *et al.*[5] on single crystals.

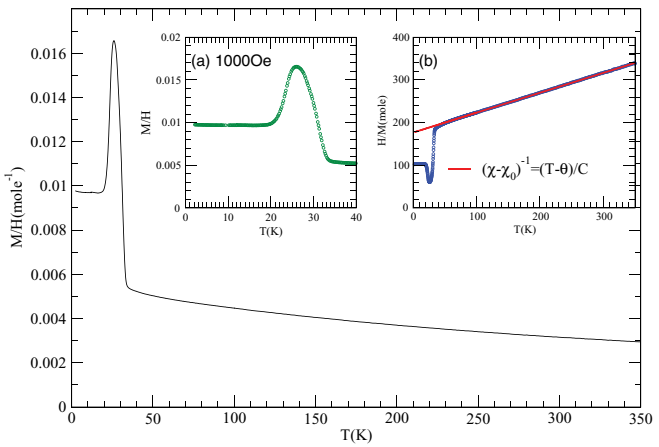

FIG. 2. (Color online) Magnetic susceptibility versus temperature showing a prominent peak at ∼26 K. By fitting with a Curie-Weiss expression, one finds that the high-temperature moment $\mu_{\rm eff} = 4.15\mu_B$/f.u. is consistent with a charge state close to $+5$. Θ is found to be -380 K.

B. ^{99}Ru Mössbauer spectra (MS)

1. *Temperature dependence*

We divide the temperature dependence of the MS into low- and high-temperature regimes. There is a modest sample-dependent variation in the temperatures defining these regimes. In the low-temperature regime, the MS show evidence of static magnetic order. However, above ∼25 K, interpretation of the MS is ambiguous and we discuss two possible ways in which to describe it.

(i) *Low Temperatures*. For temperatures in the 4–25 K range, the spectra are fit assuming a single site: all Ru sites are identical (Fig. 4). There is almost no temperature dependence with $B_{\rm hyper} = 57.8$ T. In this sample, there is no indication in the MS of a nonmagnetic impurity phase or a ferromagnetic $SrRuO_3$ contribution. The single-site fit to the 20 K is reasonable but that to the 25 K is poor, which is the boundary between the low- and high-temperature regimes. Parameter values for the fits are given in Table I. Note also a rapid decrease in $H_{\rm hyper}$ from 52.3 T at 20 K to 35 T at 25 K. There is no electric quadrapole

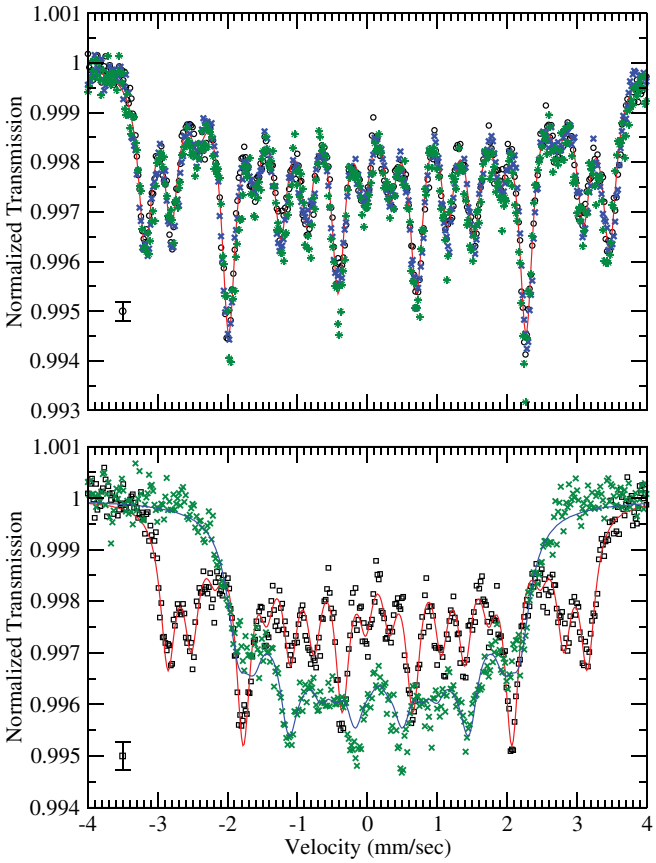

FIG. 4. (Color online) MS of Sr_2YRuO_6 at 4.2 K (○) and 10 K (∗) with the fit to the 4.2-K spectrum (full line) are shown in the upper figure. MS at 20 K (□) and 25 K (×) are shown in the lower figure. The isolated symbols in the lower-left-hand corner in each figure indicate the size of the standard error in the data.

interaction (EQI) contribution to fits at these temperatures, indicating that the RuO_6 octahedra are undistorted. This is further supported by our electronic-structure calculations,[18] based on local spin density approximation (LSDA), which found an antiferromagnetic ground state in agreement with the earlier work of Mazin and Singh.[19] The calculated electric field gradients (EFG) would lead to energies much smaller than the width of the lines in the data. The calculated EFG at the Y sites show that YO_6 octahedra are also undistorted. The isomer shift is ≃0.15 mm/sec, which is in agreement with that measured earlier in Sr_2YRuO_6 (Ref. 1) and in $Sr_2YRu_{0.95}Cu_{0.05}O_6$ (Ref. 8). This is consistent with an Ru

TABLE I. Fit parameters hyperfine magnetic field [$H(T)$], half-width at half-maximum (Γ), and isomer shift (IS). There is no electric quadrapole contribution to the fits.

	B_{hf} (T)	Γ(mm/sec)	IS (mm/sec)
4.2 K	57.8	0.118	0.142
7.5 K	57.8	0.118	0.142
10 K	57.48	0.118	0.144
15 K	56.033	0.124	0.15
20 K	52.31	0.128	0.146
25 K	35.07	0.188	0.162

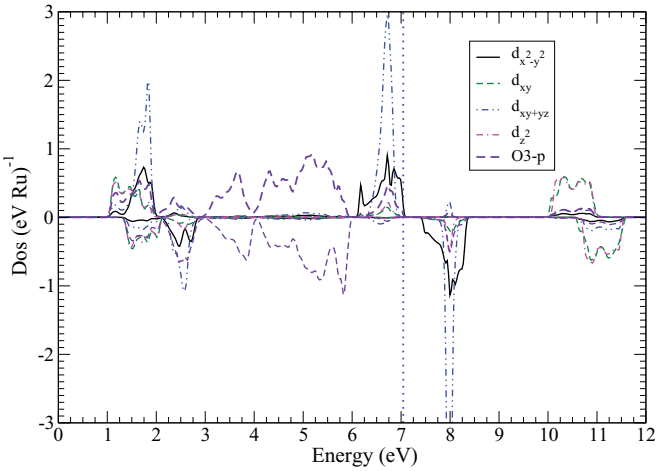

FIG. 5. (Color online) Contributions to the density of states near the Fermi energy $E_F = 7.04$ V (shown by the vertical dotted line). The sharp features on either side of E_F have contributions to the majority (above the line) and minority (below the line) spin density of states from Ru d_{xz}, d_{yz}, and $d_{x^2-y^2}$ orbitals and the O p orbitals.

charge state close to $+5$, as was assumed previously.[1,2,4] The assignment of a $+5$ charge state to Ru is based on charge counting and assumes an ionic model for the material. The isomer shift in antiferromagnetically ordered ruthenates lies between 0.0 and 0.15 mm/s, as opposed to negative values between -0.18 and -0.35 mm/s for the $+4$ charge state.[20] However, these charge-state values are only nominal. The LSDA calculations by Mazin and Singh[19] earlier showed that the polarized electrons are shared between the Ru site and its oxygen neighbors so that only 60% of the moment is in Ru-derived orbitals. The strong hybridization of the RuO bonds is typical of the ruthenates. The corresponding spin state is $S \simeq \frac{3}{2}$, which is consistent with the value found by Battle *et al.* and LSDA calculations. The magnetic hyperfine field at the Ru nucleus is due to the moment on the Ru site. The values of B_{hf} and the Ru moment found here are similar to those in $RuSr_2GdCu_2O_8$, which is an antiferromagnetic as well as superconductor at low temperatures.[20]

In Fig. 5, the calculated contributions to the density of states from Ru d orbitals and p orbitals from one of the nearest neighbor O's are shown close to the Fermi energy $E_F = 7.04$ eV, which is indicated by the dotted vertical line. The majority- and minority-spin contributions are above and below the horizontal axis, respectively. The d orbitals are split in this compound so that some of the d_{xy} and d_{z^2} orbitals at ∼10 eV for majority spins lie above the Fermi energy and are unoccupied. This is the reason that the moment is reduced compared to values estimated assuming isolated atoms. Integrating the d-orbital contribution up to E_F, one finds ∼1.7 states. Assuming orbital momentum quenching and $g = 2$, one finds a moment close to that derived from neutron scattering.[4] Indeed, the overlap of contributions from Ru d-orbital and O p-orbital contributions between 6 and ∼8 eV and again between 10 and 11.5 eV is evidence of the strong hybridization of these orbitals pointed out by Mazin and Singh.[19]

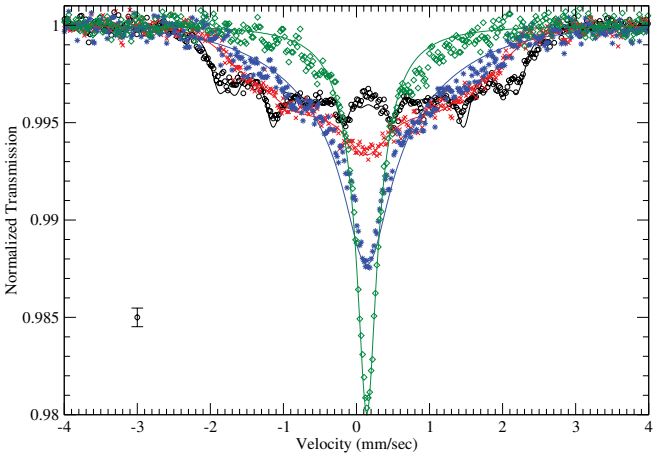

FIG. 6. (Color online) MS of Sr_2YRuO_6 at 25 K (○), 26.5 K (×), 27.5 K (∗), and 28 K (◊). The lines through the data are fits based on the motional narrowing model discussed in the text. The isolated symbol in the lower-left-hand corner in the figure indicates the size of the standard error in the data.

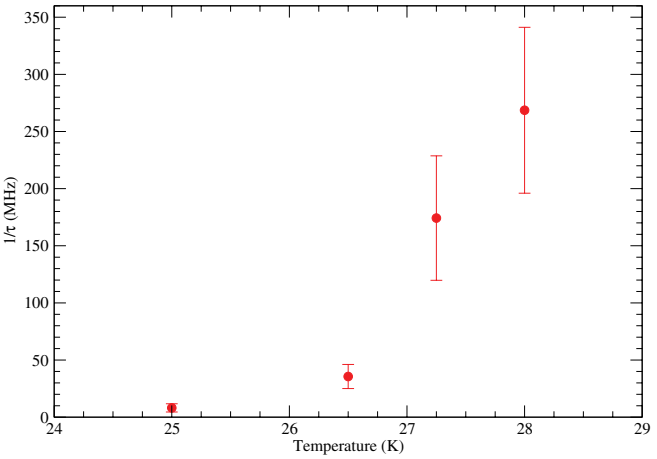

FIG. 7. (Color online) Temperature dependence of $\frac{1}{\tau}$.

(ii) *High-temperature region*. Between ∼25 and 28 K, the MS evolves into a single peak. There is a sharp drop in the hyperfine field between 20 K (52 T) and 25 K (35 T). As a result of the reduction in width of the 25 K spectrum, some of the lines seen at 20 K can no longer be resolved and a peak develops at ≃0.15 mm/s (Fig. 6). There is some sample dependence. In the MS shown, here the temperature region is between 25 and 28 K, while for another sample it is between 25.3 and 30 K. The MS at 28 K can be fit fairly well with a simple Lorentzian line and is very similar to that at 30 K, which is essentially identical to that at 34 K. The best fit to the MS at 30 K is a single line, indicating that there is no static magnetic order beyond 28 K. We have considered two different models for this temperature dependence of the MS. In the first model, the evolution of the MS is due to random fluctuations in the direction and a reduction in magnitude of the hyperfine field as temperature increases so that by ∼28 K the rate of fluctuation is too fast for the Mössbauer transitions to follow. In the second model, the MS are due to static magnetic order in regions of different sizes which leads to a temperature-dependent distribution of hyperfine fields which shrink to values close to zero so that there is no evidence of static magnetic order by 28 K.

The fluctuation model is due to Bloom and co-workers.[21,22] The direction of $B_{\text{hyperfine}}$ switches randomly between different directions at a rate $\frac{1}{\tau}$, so that the there are two parameters in the model B_{fl}, the magnitude of the fluctuating hyperfine field and τ. The intrinsic linewidth is set to that of the single-line spectra at 30 and 35 K, $\Gamma_o = 0.23$ mm/s. The Hamiltonian describing the system in a given nuclear state (ground, $n = gr$, or excited, $n = ex$) is

$$H = -g_n\mu_n \sum_{j=1,N} H^j_{fl} I_j f_j(t), \qquad (1)$$

where g_n is the gyromagnetic factor of the nuclear state, μ_n is the nuclear Bohr magneton, the sum runs over the N directions among which the hyperfine magnetic field fluctuates, I_j is the component of the nuclear spin along direction j, and $f_j(t)$ is a random function of time with values corresponding to different directions. There is no correlation between the directions of the fluctuating hyperfine magnetic field, and this is incorporated in the calculation through a random phase treatment in averaging over the possible changes in directions j and a trace over the product space of the nuclear states $|I_{gr}m\rangle|I_{ex}m'\rangle$.[22] For the ^{99}Ru nucleus, $I_{gr} = \frac{5}{2}$ and $I_{ex} = \frac{3}{2}$. We considered the case of two-dimensional fluctuations in which the direction flipped between two mutually perpendicular directions $\pm\hat{x}$ and $\pm\hat{y}$ and the case of three dimensions $\pm\hat{x}$, $\pm\hat{y}$, and $\pm\hat{z}$. We found that the two-dimensional model gave better fits.

The full lines in Fig. 6 are fits to the MS based on this model. The corresponding values of $\frac{1}{\tau}$ are shown in Fig. 7 and those of B_{fl} are shown in Fig. 9. The value of B_{hf} from the single-site static model at 25 K is essentially the same as B_{fl} (≃36 T) and $\frac{1}{\tau}$ is found to be 8.8 MHz. As temperature increases, $\frac{1}{\tau}$ changes rapidly and at 28 K, $\frac{1}{\tau}$ ∼250 MHz and B_{fl} has fallen to ≃22 T. The uncertainty in the value of $\frac{1}{\tau}$ from the best fits increases because the fits are increasingly insensitive to the value of $\frac{1}{\tau}$ as the MS narrows to a single line.

In the static field model, regions without static magnetic order develop, as well as a distribution of hyperfine magnetic fields. The calculated line through the 26.5 K data is averaged over a set of MS calculated using a distribution of hyperfine fields $f(B_{hf})$, shown in Fig. 8. At 26.5 K, the distribution of hyperfine fields is strongly peaked at 30 T. At 28 K, $f(B_{hf})$ is peaked at $B_{hf} = 0$. The $f(B_{hf})$ are consistent with the formation of smaller regions of static magnetic order with a range of sizes as long-range order is lost with increasing temperature. The average value of B_{hf} is given in Fig. 9.

The data do not allow us to discriminate between the two models and we postpone further consideration of the explanation until the Sec. IV.

2. *Temperature dependence of* $B_{\text{hyperfine}}$

The temperature dependence of the hyperfine field can be analyzed in terms of the magnon spectrum at low temperatures. From Fig. 4 the hyperfine field is independent of temperature up to ∼10 K. This points to a gap in magnon spectrum which results in the absence of thermally activated magnons. We use the nearest-neighbor (NN) Heisenberg model on a fcc lattice of Kuz'min *et al.*[23] for the magnon spectrum. This model,

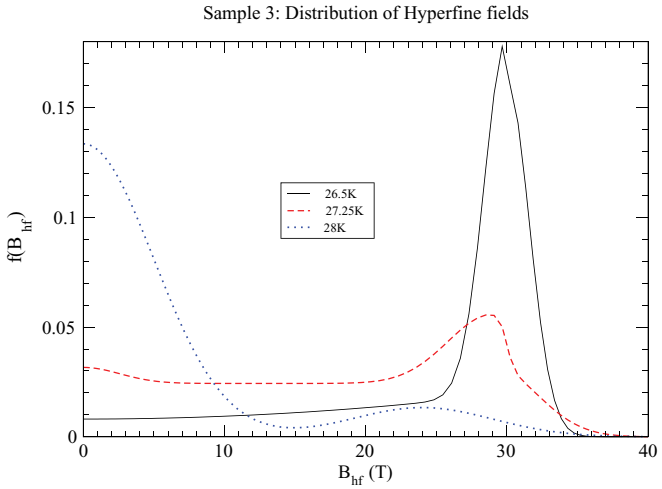

FIG. 8. (Color online) The distribution of hyperfine fields at different temperatures in the transition region.

based on the neutron scattering data of Battle and Macklin, is used to fit the temperature dependence. Although there are 12 NN sites on the fcc lattice, the lowest energy per site in the classical ground state is -4 J, instead of -12 J, because of the connectivity of the fcc lattice. The magnon spectrum $\varepsilon(\vec{q})$ is calculated in the linear spin wave approximation about this frustrated ground state and disperses with a linear dependence on q_z at low energies. This one-dimensional spectrum arises from the frustration between NN bonds in the classical ground state of the model and ensures that there is no order at $T > 0$, independent of the size of the NN Heisenberg coupling. Kuz'min *et al.* introduced magnetic anisotropy in their model $J_\parallel > J_\perp$ to pick a mean-field ground state consistent with the moments lying in the YRuO planes found by Macklin and Battle. This also introduces a gap in the magnon spectrum

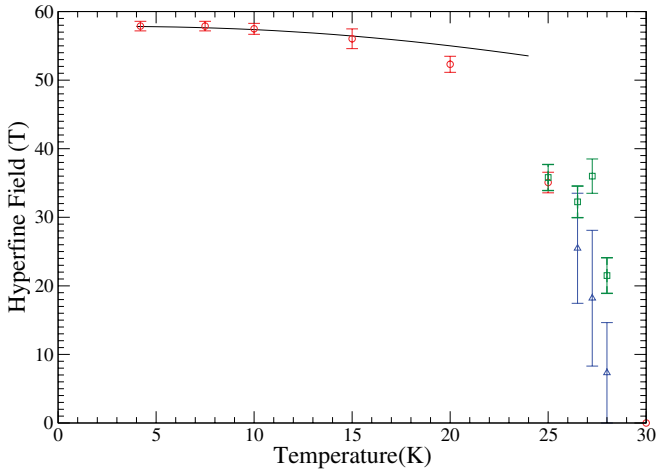

FIG. 9. (Color online) Hyperfine fields as a function of temperature. The error bars for values from single fits (○) and from the motional narrowing model (□) are determined by doubling the sum of the square of the difference between the data and the calculated spectrum found in the best fit to the data. The values from distributions of hyperfine fields (△) are the average value and the standard deviation of the distribution. The full line is the fit to the low-temperature data based on the magnon spectrum of Kuz'min *et al.*[23] discussed in the text.

which suppresses thermal activation of magnons and makes magnetic order at $T > 0$ possible.

In Fig. 9, we fit the calculated temperature dependence of the hyperfine field $H(T) = H(0)[1 - \sum_{\vec{q}} n(\varepsilon_{\vec{q}})]$, where $n(\varepsilon_{\vec{q}})$ is the Bose-Einstein distribution, using their expression for $\varepsilon(\vec{q})$ with parameter values $J = \frac{1}{2}(J_\parallel + J_\perp) = 150$ K and $J_\parallel - J_\perp = DJ = 1$ K. This gives the gap in the magnon spectrum $\simeq$15 K. It has been shown that next-nearest-neighbor (NNN) coupling λJ in a Heisenberg model on a fcc lattice can also stabilize magnetic order at finite temperatures by giving the magnon spectrum three-dimensional character.[24,25] Kuz'min *et al.* estimated λ to be $\sim 10^{-2}$. However, isotropic interactions do not lead to a gap in the magnon spectrum. Including both anisotropy and NNN coupling, the long-wavelength magnon dispersion becomes $\simeq \frac{2J\bar{S}}{3}\sqrt{D + \frac{1}{4}(q_z^2 + \lambda|\vec{q}|^2)}$, where $\bar{S} = 1.85\mu_B$, which is the value of the ordered moment found by Battle and Macklin. Given the values of D and λ above, the effect of the NNN coupling on low-temperature properties is much smaller than that of anisotropy.

3. *Applied magnetic fields*

The MS of Sr_2YRuO_6 was measured at different temperatures in 3 and 5 T fields. The MS at 4.2 K are shown in Fig. 10. The sample used in these measurements contained a RuO impurity phase. The dashed lines in the figure are the contribution to the spectra from this impurity phase at different applied magnetic fields, calculated from the form of the zero-field spectrum.[26] The impurity phase contains $\sim$2% of the Ru's in the sample from the ratio of the integrated weights beneath the curves, so that the impurity phase is less than 1% of the sample by volume. The magnetic anisotropy responsible for the gap in the magnon spectrum also ensures that the moments are not free to respond to the external field for the field strengths used here. Consequently, the spectra are the result of an average of the spectra from each crystallite whose internal ordered field is randomly orientated with respect to the direction of the external field, which is also the direction of propagation of the incident γ rays. The MS in Fig. 10(a), in the absence of an applied field, is the average over relative orientations for a powder sample. The large peaks at $\sim \pm 2$ mm/s are due to $\Delta m = \pm 1$ transitions, which are the only allowed transition when the direction of the ordered moments are aligned parallel or antiparallel with the direction of the incident γ ray. Naively, one would expect the effective fields at the Ru nucleus to be 57.7 ± 3 T or 57.7 ± 5 T in these applied fields, which would split the this peak into two. This clearly is not seen in the data. Therefore, in averaging over θ, the angle between the ordered moments in the absence of the field and the direction of the applied field, we have included a factor $1 - \cos^6\theta$, which suppresses the component of the applied field along the direction of the moments in the ferromagnetically ordered planes. The form of this factor was determined by looking at the best fits. This additional factor could arise in a model where the moments are saturated along the directions of ferromagnetic order in each plane and are locked together within domains so that they act as a single large moment. In this case, when the field is applied parallel to the zero-field direction of the ordered moments, the spin polarization of electrons at the Ru site and

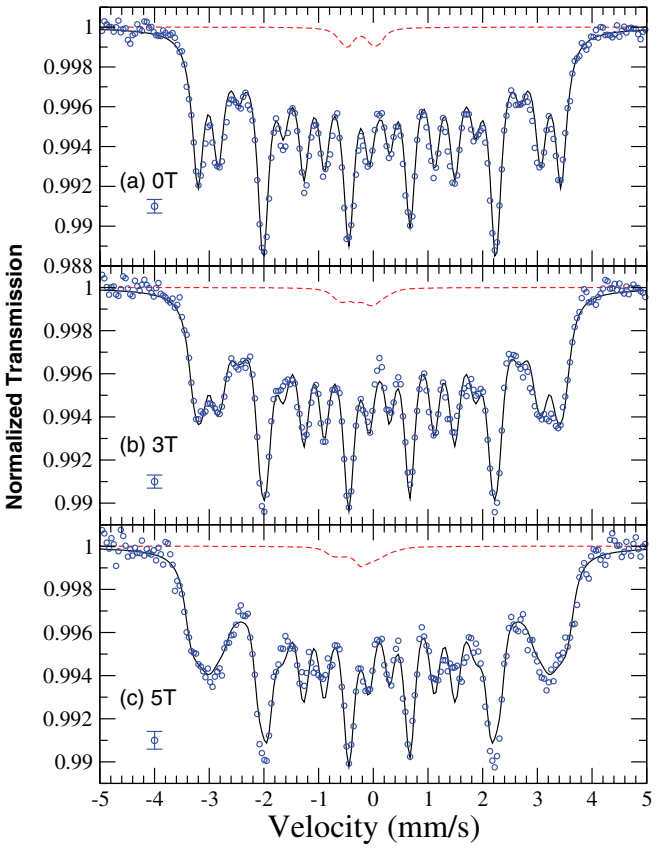

FIG. 10. (Color online) MS of Sr_2YRuO_6 at 4.2 K in (a) zero applied field, (b) 3 T, and (c) 5 T. The full lines are fits calculated by averaging over the relative orientations between the internal ordered field in each crystallite and the direction of the applied field/direction of propagation of the incident γ ray. The dashed line is the contribution of the RuO impurity in the sample at each field. The isolated symbols in the lower-left-hand corner in each figure indicate the size of the standard error in the data.

the resulting hyperfine magnetic field are independent of the applied field until it is sufficiently strong to cause a spin-flop transition.[27] Net moments are induced when the external field is applied along other directions, as is seen in the magnetization data (Fig. 3). In agreement with Cao *et al.*,[5] we do not see the spin-flop transition reported by Battle and Macklin[4] in magnetic susceptibility for a 3.8 T applied field. It would be surprising if a 5 T applied field could be responsible for such a transition, given that the magnitude of the gap in the magnon spectrum is ∼15 K from the fit to the temperature dependence of the hyperfine field.

Just as in the absence of an applied field there is very little temperature dependence up to ∼12 K when a 5 T field is applied. At 25.3 K, the width of spectrum is much narrower and the distinguishing features between zero field and 3 T seen at 4.2 K can no longer be resolved.

IV. DISCUSSION

The same discrepancy in ionic radii of the Ru and rare-earth atoms holds when Y is substituted with rare-earth lanthanides. The similarities between different members of this class of ruthenates are striking. Specific-heat measurements reported here confirm the second phase transition in Sr_2YRuO_6 reported by Singh and Tomy[14] and by Bernardo *et al.*[15] Two transitions, close together in temperature, have also been reported in Sr_2LuRuO_6.[28] However, our measured MS show that this transition is not associated with a transition from a static magnetically ordered state, contrary to the suggestion of Singh and Tomy. Instead, the MS between the two transitions at ∼26 and ∼30 K can be interpreted as either due to motional narrowing or to the development of a distribution of hyperfine fields with increasing temperature.

There is no evidence of the transition at ∼30 K in the MS. The motional narrowing explanation is that the electronic moment at the Ru sites fluctuates too rapidly at these temperatures for transitions between nuclear states of the Ru nucleus to follow. The characteristic differences in the ^{99}Ru nuclear energy levels with $B_{hf} \simeq 60$ T correspond to fluctuations ∼30 MHz. Beyond this scale, fluctuations of the hyperfine field start to degrade the peaks in the ^{99}Ru MS and by ∼50 MHz the ^{99}Ru MS collapses to a single line.[29] In the case of Sr_2YRuO_6, the MS show that the average hyperfine magnetic field decreases rapidly so that this frequency threshold is also decreasing. One candidate for the origin of this effect is the coupling between structural and magnetic properties of Sr_2YRuO_6. The insulator ground state of Sr_2YRuO_6 is due to the tilting of the octahedra.[19] In LDA calculations, the absence of the tilting leads to itinerant antiferromagnetic ground states at $T = 0$ rather than an insulator. The coupling between moments is due to superexchange through two oxygen atoms, one in each octahedra of the two Ru atoms and both in their common neighboring YO_6 octahedron. In these circumstances, it is clear that there is a strong coupling between magnetic order and thermally activated tilting modes of the octahedra. It would not be surprising if this coupling leads to fluctuations of the ordered moments responsible for the hyperfine magnetic field at the Ru site.

The second interpretation of the MS in the transition region is that microscopically large regions of static magnetic order break up into smaller domains of static magnetic order, which leads to a distribution of hyperfine fields. The dimensions of these smaller domains determine the strength of magnetic correlations and the magnitude of the hyperfine field at Ru sites. Eventually, the characteristic value of the B_{hf} becomes so small that the MS are indistinguishable from single-line spectra.

Both explanations of the development of short-range correlations above 26 K are consistent with aspects of the recent neutron diffraction results on Sr_2YRuO_6 of Granado *et al.*[16] However, the evidence of magnetic moments above 28 K in their data suggests that the motional narrowing is more consistent with both experiments.

The second transition seen in the specific-heat data at ∼30 K is well defined. However, there is no corresponding strong feature in the magnetization where a broad peak develops starting at ∼32 K with a maximum at ∼26 K, the temperature at which the first peak in the specific heat is seen. This suggests that the transition at ∼30 K is not a second-order transition to static magnetic order and this is consistent with the results of the Mössbauer measurements.

A correspondingly broad single feature is also seen in the susceptibility at the transition to antiferromagnetism in another ruthenate, $Ba_3CoRu_2O_9$.[30] Although Granado *et al.*[16] detect the structural anomalies, which Bernardo *et al.* associated with the phase transitions at 24 and 30 K, they do not identify these with a structural transition. However, the emergence of purely magnetic reflections near 32 K clearly suggests the onset of magnetic order, which they suggest is partially frustrated. In contrast, the MS data show a deterioration of static long-range magnetic order starting at ∼25 K and its complete absence beyond ∼28 K, suggesting the fluctuation rate of moments at ∼28 K exceeds the integration ability for the MS measurements, while being slow enough for interaction with neutrons. Bernardo *et al.*[15] have found evidence of structural transitions at both 24 and 30 K using thermal expansion and x-ray powder diffraction. Given that the MS show that there are no sharp magnetic transitions at 24 and 30 K, the sharp features seen in the specific heat seem to come from subtle structural transitions which have the effect of destroying the static long-range magnetic order present below 24 K.

Our results also give information on the magnitude of the exchange constant and the degree of anisotropy in the localized magnetic moment analysis of Sr_2YRuO_6's magnetic properties. The size of the nearest-neighbor exchange coupling found from our fit to temperature independence of the hyperfine field at temperatures $\leqslant 10$ K, $J = 150$ K, is $\simeq \frac{1}{2}$ the value estimated by Kuz'min *et al.* from a comparison of simplified tight-binding expressions for J with calculations of energy differences from linearized augmented plane wave (LAPW) calculations.[19] The gap in the magnon spectrum, $\simeq$15 K, arises from a ∼1% difference in the exchange constants in the model of Kuz'min *et al.*[23] It will be difficult to determine unambiguously the source of the small degree of magnetic anisotropy in the system from *ab initio* calculations.

In conclusion, we have shown that the transition from static magnetic order in Sr_2YRuO_6 begins at ∼24 K and it takes place over a temperature range of ∼1–2 K. It remains to be seen what the nature of the magnetic transition is in Sr_2LnRuO_6, where Ln has a magnetic moment, unlike Y and Lu, and whether there is a second transition present. The presence of a magnetic moment on the Ln site would provide an additional interaction path between the Ru moments. How this would affect the nature of the transitions in these materials remains to be determined.

ACKNOWLEDGMENTS

Sample synthesis, thermodynamic and transport measurements at SDSU were supported by Grant No. NSF-DMR-085335. Preparation of the ^{99}Ru sources and the Mössbauer measurements and their analysis were supported by Grant No. USDOE(DE-FG02-03ER46064) at BSC.

*coffeyd@buffalostate.edu

[1] R. Greatrex, W. N. Greenwood, M. Lai, and I. Fernandez, J. Solid State Chem. **30**, 137 (1979).
[2] Y. Doi and Y. Hinatsu, J. Phys.: Condens. Matter **11**, 4813 (1999).
[3] V. P. S. Awana, R. Tripaathi, V. K. Sharma, H. Kishan, E. Takayama-Muromachi, and I. Felner, J. Magn. Magn. Mater. **312**, 290 (2007).
[4] P. D. Battle and W. J. Macklin, J. Solid State Chem. **52**, 138 (1984).
[5] G. Cao, Y. Xin, C. S. Alexander, and J. E. Crow, Phys. Rev. B **63**, 184432 (2001).
[6] M. K. Wu, D. Y. Chen, D. C. Ling, F. Z. Chien, S. R. Sheen, D. C. Ling, C. Y. Tai, D. H. Chen, and F. C. Zhang, Z. Phys. B: Condens. Matter **102**, 37 (1997).
[7] M. K. Wu, D. Y. Chen, D. C. Ling, and F. Z. Chien, Phys. B (Amsterdam) **284–288**, 477 (2000).
[8] M. DeMarco, H. A. Blackstead, J. D. Dow, M. K. Wu, D. Y. Chien, F. Z. Chien, M. Haka, S. Toorongian, and J. Fridmann, Phys. Rev. B **62**, 14301 (2000).
[9] D. R. Harshman, W. J. Kossler, A. J. Greer, D. R. Noakes, C. E. Stronach, E. Koster, M. K. Wu, F. Z. Chien, J. P. Franck, I. Isaac, and J. D. Dow, Phys. Rev. B **67**, 054509 (2003).
[10] E. Galstyan, Y. Y. Xue, M. Iliev, Y. Sun, and C. W. Chu, Phys. Rev. B **76**, 014501 (2007).
[11] E. Galstyan and Y. Xue, Phys. Rev. B **79**, 016502 (2009).
[12] I. Nowik and I. Felner, J. Magn. Magn. Mater. **237**, 1 (2001).
[13] R. Kumar, C. V. Tomy, P. L. Paulose, and R. Nagarajan, J. Appl. Phys. **97**, 10A907 (2005).
[14] R. P. Singh and C. V. Tomy, Phys. Rev. B **78**, 024432 (2008).
[15] P. L. Bernardo, L. Ghivelder, G. G. Eslava, H. S. Arouim, E. H. C. Sinnecker, I. Felner, J. J. Neumeier, and S. Garcia, J. Phys.: Condens. Matter **24**, 486001 (2012).
[16] E. Granado, J. W. Lynn, R. F. Jardim, and M. S. Torikachvili, Phys. Rev. Lett. **110**, 17202 (2013).
[17] M. DeMarco, G. Cao, J. E. Crow, D. Coffey, S. Toorongian, M. Haka, and J. Fridmann, Phys. Rev. B **62**, 14297 (2000).
[18] P. Blaha, K. Schwarz, G. K. H. Madsen, Kvasicka and J. Lutz, WIEN2K:*Augmented Plane Wave + Local Orbitals Program for Calculating Crystal Properties* (Technische Universität Wien, Wien, Austria, 2001).
[19] I. I. Mazin and D. J. Singh, Phys. Rev. B **56**, 2556 (1997).
[20] D. Coffey, M. DeMarco, B. Dabrowski, S. Kolesnik, S. Toorongian, and M. Haka, Phys. Rev. B **77**, 214412 (2008).
[21] M. Blume and J. A. Tjon, Phys. Rev. **165**, 446 (1968).
[22] S. Dattagupta, Phys. Rev. B **16**, 158 (1977).
[23] E. V. Kuz'min, S. G. Ovchinnikov, and D. J. Singh, Phys. Rev. B **68**, 024409 (2003).
[24] D. ter Haar and M. E. Lines, Philos. Trans. R. Soc. London, Ser. A **255**, 1 (1962)
[25] M. E. Lines, Proc. R. Soc. London **271**, 105 (1963).
[26] D. C. Foyt, M. L. Good, J. G. Cosgrove, and R. L. Collins, J. Inorg. Nucl. Chem. **37**, 1913 (1975).
[27] B. Dieny, J. P. Gavigan, and J. P. Rebouillat, J. Phys.: Condens. Matter **2**, 159 (1990).
[28] R. P. Singh and C. V. Tomy, Solid State Commun. **150**, 804 (2010).
[29] P. Gütlich, R. Link, and A. Trautwein, *Mössbauer Spectroscopy and Transition Metal Chemistry* (Springer-Verlag, Berlin, 1978), Sec. 6.7.
[30] H. D. Zhou, A. Kiswandhi, Y. Barlas, J. S. Brooks, T. Siegrist, G. Li, L. Balicas, J. G. Cheng, and F. Rivadulla, Phys. Rev. B **85**, 041201(R) (2012).